We can also compare the ratio of k_2 to k_1. In this case, all of the determined ratios are in fair agreement. Our ratio of 9.0 compares well to Pilling (8.3), Temps (11.2), and Laufer (10.7). Vinckier, who measured these rates relative to $O + {}^3CH_2$, obtains a value of 12.5, which is somewhat further from our value.

A number of determinations of k_3 have been made. The earlier works by Vinckier et al.,[13] Homann et al.,[14] and Laufer et al.[10] indicated k_3 to be on the order of 1×10^{-12} cm^3 molecule^{-1} s^{-1}. This value is substantially larger than one might expect based on conventional triplet carbene reactivity. A more recent determination of k_3 by Walsh et al.[15] gave a much smaller value for this rate constant. Utilizing a laser flash photolysis gas chromatographic end product analysis, they derived an upper limit of 1×10^{-15} cm^3 molecule^{-1} s^{-1}. Finally, Bohland et al.[16] in a direct measurement of CH_2 in an LMR/flow system recently have reported that k_3 is less than 8×10^{-16} cm^3 molecule^{-1} s^{-1}. Our direct observation of $k_3 < 1.4 \times 10^{-14}$ cm^3 molecule^{-1} s^{-1} by an independent method conclusively verifies that k_3 is much smaller than earlier thought.

Conclusion

In this study we have used infrared diode laser absorption flash kinetic spectroscopy to measure the reaction rates of ${}^3CH_2$ with O_2, NO, and C_2H_2. Our measured rates are generally in good agreement with other direct measurements of these rates and in disagreement with the results of indirect studies.

In these experiments we have seen that, in the absence of added reactant gases, ${}^3CH_2$ is eventually consumed in a recombination reaction. In principle, then, we should have a measure of the recombination rate of ${}^3CH_2$ through analysis of decays in the absence of reactive gases. However, the recombination reaction of ${}^3CH_2$ is described by second-order reaction kinetics. Analyzing second-order kinetic processes requires that the absolute concentration of ${}^3CH_2$ radicals be known. Unfortunately, in these experiments we do not believe that we can precisely define the density of ${}^3CH_2$ species in our probe volume. We are currently proceeding with a measurement of this recombination rate.

We also have not addressed important questions with respect to the products of the reactions studied. With the flexibility in tunability of our diode laser spectrometer system, we should be able to study the rises of any molecular products (except homonuclear diatomics) by direct time-resolved absorption. Studies of this nature are also in progress.

Acknowledgment. We thank Bill Green and Steve Prodnuk for their assistance during various phases of this work. We also thank F. Temps for sending us results prior to publication. Use of an excimer laser borrowed from the San Francisco Laser Center during the early phases of this work is acknowledged. This research was supported by the Director, Office of Energy Research, Office of Basic Energy Sciences, Chemical Sciences Division of the U.S. Department of Energy, under Contract DE-AC03-76SF00098. C.B.M. acknowledges assistance from the Miller Foundation in the form of a Miller Research Professorship.

Registry No. CH_2, 2465-56-7; O_2, 7782-44-7; NO, 10102-43-9; C_2H_2, 74-86-2; C_2H_2O, 463-51-4.

Rate Coefficient for the H + NF(a$^1\Delta$) Reaction

Steven J. Davis, Wilson T. Rawlins, and Lawrence G. Piper*

Physical Sciences Inc., Dascomb Research Park, P.O. Box 3100, Andover, Massachusetts 01810
(Received: December 29, 1987)

We have measured the rate coefficient of the reaction between atomic hydrogen and NF(a$^1\Delta$) in a discharge-flow reactor by monitoring the decay of NF(a$^1\Delta$) in excess hydrogen atoms. Reacting H_2 with the effluents of a low-power discharge through NF_3/Ar mixtures produced the NF(a). It was monitored in fluorescence at 874 nm. A thermally stabilized discharge in H_2/Ar mixtures generated the atomic hydrogen. The chemiluminescent titration of H with NOCl determined H atom number densities. The measured value is $(3.1 \pm 0.6) \times 10^{-13}$ cm^3 molecule^{-1} s^{-1}. These results are necessary to evaluate the potential efficiency of a proposed scheme for generating metastable nitrogen beginning with the addition of atomic hydrogen to NF_2.

Introduction

The lowest lying metastable state of N_2, $A^3\Sigma_u^+$, is a well-known energy reservoir (~6 eV) which has potential as an energy storage candidate for use in short-wavelength laser systems. As such, knowing the means to generate this species efficiently and understanding its energy-transfer kinetics in the lasing medium are essential requirements for laser device design. Several laboratory investigations have identified methods for forming $N_2(A)$ chemically. Two methods, in particular,[1-5] may be capable of producing $N_2(A)$ in sufficient quantities to drive a transfer laser. The first method consists of a set of reactions initiated by the reaction of atomic hydrogen with NF_2 and appears to involve the metastables NF(a$^1\Delta$) and N(^{2}D) as key intermediate species.[1-3] An intriguing second method is the bimolecular disproportionation of the highly energetic azide radical, N_3.[4,5] The former method has a potentially high efficiency per unit mass, but it requires the handling of the hazardous species N_2F_4 (the thermal source of NF_2) and may present serious kinetic complications upon scale-up from laboratory experiments. The latter method, which uses ionic metal azides such as NaN_3 as thermal sources of N_3 radicals, is also potentially mass efficient.

This paper is concerned with one aspect of excited molecular nitrogen production from the H + NF_2 reaction sequence. This reaction has been the subject of several previous studies, and its history in the literature is intriguing. The first report was by Clyne and White in 1970.[6] They observed that the reaction of H + NF_2 produced NF(a$^1\Delta$), NF(b$^1\Sigma$), and N_2(B$^3\Pi_g$). They thought that recombination of N(^{4}S) atoms was the source of N_2(B).

* Author to whom correspondence should be addressed.

(1) Cheah, C. T.; Clyne, M. A. A.; Whitefield, P. D. *J. Chem. Soc., Faraday Trans. 2* **1980**, *76*, 711.
(2) Cheah, C. T.; Clyne, M. A. A. *J. Chem. Soc., Faraday Trans. 2* **1980**, *76*, 1543.
(3) Cheah, C. T.; Clyne, M. A. A. *J. Photochem.* **1981**, *15*, 21.
(4) Piper, L. G.; Taylor, R. L., PSI TR-96, prepared for the Department of Energy under Contract EY-76-C-02-2960, *000, 1977.
(5) Piper, L. G.; Krech, R. H.; Taylor, R. L. *J. Chem. Phys.* **1979**, *71*, 2099.
(6) Clyne, M. A. A.; White, I. F. *Chem. Phys. Lett.* **1970**, *6*, 465.

0022-3654/89/2093-1078$01.50/0

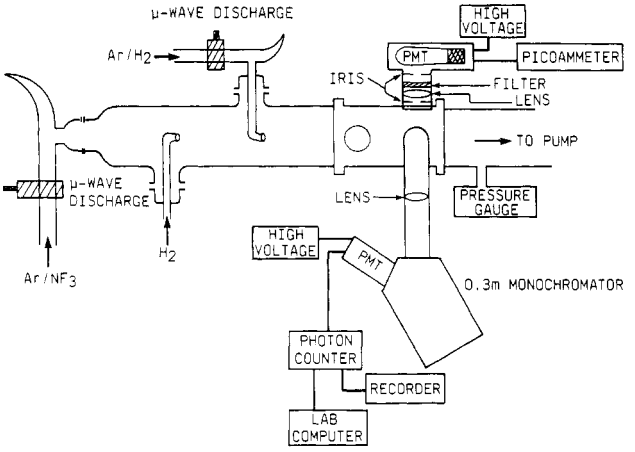

Figure 1. Block diagram of the flow tube.

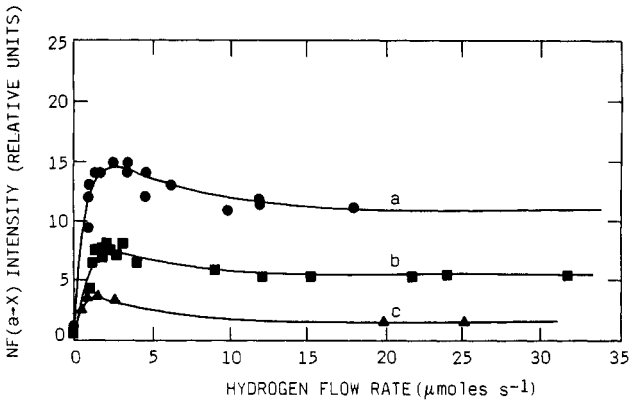

Figure 2. Relative concentration of NF(a) as a function of H_2 flow for three different NF_3 flows: (a) 6 μmol s^{-1}, (b) 2.7 μmol s^{-1}, and (c) 1.25 μmol s^{-1}.

In 1973 Herbelin and Cohen[7] performed a similar chemiluminescence study and suggested the following mechanism:

$$H + NF_2 \rightarrow NF(a) + HF \quad (1)$$

$$H + NF(a) \rightarrow N(^2D) + HF \quad (2)$$

$$N(^2D) + NF(a) \rightarrow N_2(B) + F \quad (3)$$

Although they could not prove this model, they presented indirect evidence for its validity and argued that spin and angular momentum conservation would be major determinants in reaction product channel availability. In particular, they emphasized that the reaction of H with NF(a) would produce $N(^2D)$ exclusively if these correlation rules held rigorously. In spite of these early observations, the reaction mechanism for this potentially important source of N_2^* has remained unclear.

In the early 1980s Clyne and co-workers published a series of detailed experiments designed to clarify this interesting reaction sequence.[1-3] Using sensitive diagnostic techniques, they observed that $N(^2D)$ apparently was the primary product of reaction 2 and concluded that Herbelin and Cohen's proposed mechanism probably was correct. In addition, they determined a rate coefficient for reaction 1 (H atom removal by NF_2) of $(1.5 \pm 0.2) \times 10^{-11}$ cm^3 $molecule^{-1}$ s^{-1} and estimated the rate coefficients of reactions 2 and 3 to be 2.5×10^{-13} and 7×10^{-11} cm^3 $molecule^{-1}$ s^{-1}, respectively. Subsequent investigations by Malins and Setser[8] found a total rate coefficient for reaction 1 of 1.3×10^{-11} cm^3 $molecule^{-1}$ s^{-1} by observing the formation of the HF product. They also found that $\gtrsim$90% of the reaction resulted in $NF(a^1\Delta)$ formation and established a radiative lifetime for NF(a) of 5.6 s. This latter value agrees with recent theoretical calculations.[9,10]

This paper describes measurements of the rate coefficient for reaction 2. A subsequent paper[11] will describe measurements of the rate coefficient for reaction 3 and will show our results provide further evidence in favor of Herbelin and Cohen's model.

Experimental Section

Flow Tube Description. A new, modular, fast-flow reactor was constructed specifically for these experiments and is shown, schematically, in Figure 1. It is similar in most respects to another discharge-flow reactor we have described in detail.[12-15] The flow tube is constructed from 5-cm-i.d. Pyrex, and the observation region is 5-cm-i.d. stainless steel chamber coated with Teflon (DuPont Poly TFE No. 852-201). Prior to Teflon coating the entire observation chamber was painted with a flat black primer. The black primer/Teflon combination serves two functions. The primer reduces scattered light which facilitates all spectroscopic observations while the Teflon coating reduces wall reactions and recombinations.

$NF(a^1\Delta)$ is produced in the upstream end of the reactor by mixing the effluents of a weak microwave discharge ($\sim$6 W) of NF_3 dilute in argon with a substantial flow of molecular hydrogen (vide infra). Further downstream, H atoms, produced in a microwave discharge ($\sim$50 W) through a flow of H_2 and argon in a side arm, are injected into the flow. Still further downstream, the number densities of NF(a) and H are monitored by observing NF(a–X) emission at 874 nm and HNO emission at 693 nm (when NO is added to the reactor), respectively.

All gas flows are monitored by electronic mass flowmeters. The flowmeters were calibrated by measuring the change in pressure versus time of gas flows into a standard volume (6.5- or 12.0-L flasks). The pressure change was measured with a Validyne pressure transducer that had been calibrated against a mercury or oil manometer. Typical flow rates included 2000 and 400 μmol s^{-1} for the Ar through the NF_3 and H_2 discharges, respectively, 0.2 μmol s^{-1} for the NF_3, 200 μmol s^{-1} for the H_2 mixed with the NF_3/Ar discharge effluent, and 0–100 μmol s^{-1} for the H_2 through the H atom discharge.

The pressure in the flow tube is measured with a Baratron 0–10-Torr capacitance manometer. Typical flow tube pressures ranged from 0.13 to 2.5 Torr. Flow velocities varied from 500 to 5300 cm s^{-1}.

The present configuration uses two ports for optical detection. Visible and near-infrared chemiluminescence is monitored with a 0.3-m McPherson monochromator and a thermoelectrically cooled Hamamatsu GaAs photomultiplier tube. The other port has a filtered photometer for monitoring HNO emission which is used to calibrate H atom number densities (described below).

$NF(a^1\Delta)$ Production. We used the reaction of hydrogen with the products of a weak microwave discharge of NF_3 dilute in Ar to produce $NF(a^1\Delta)$. Initial runs showed that the emitting species produced by the NF_3 discharge consisted almost exclusively of NF(b→X) and NF(a→X) emissions at 528 and 874 nm, respectively. Weak N_2(B→A) first-positive emission was also observed, but since the radiative lifetime for N_2(B) is orders of magnitude shorter than those for NF(a) and NF(b), N_2(B) is a minor product.

Upon addition of molecular hydrogen to the effluents of the NF_3 discharge, the NF(a,b) emissions increased approximately an order of magnitude and the emission from N_2(B) decreased, vanishing at high H_2 flow rates. Observing enhanced NF(a)

(7) Herbelin, J. M.; Cohen, N. *Chem. Phys. Lett.* **1973**, *20*, 605.
(8) Malins, R. J.; Setser, D. W. *J. Phys. Chem.* **1981**, *85*, 1342.
(9) Bettendorff, M.; Klotz, R.; Peyerimhoff, S. D. *Chem. Phys.* **1986**, *110*, 315.
(10) Havriliak, S. J.; Yarkony, D. R. *J. Chem. Phys.* **1985**, *83*, 1168.
(11) Davis, S. J.; Piper, L. G., manuscript in preparation.
(12) Piper, L. G.; Marinelli, W. J.; Rawlins, W. T.; Green, B. D. *J. Chem. Phys.* **1985**, *83*, 5602.
(13) Piper, L. G.; Rawlins, W. T. *J. Phys. Chem.* **1986**, *90*, 320.
(14) Piper, L. G.; Cowles, L. M.; Rawlins, W. T. *J. Chem. Phys.* **1986**, *85*, 3369.
(15) Piper, L. G.; Donahue, M. E.; Rawlins, W. T. *J. Phys. Chem.* **1987**, *91*, 3883.

emission from H_2 was added to the discharge effluents indicates that, in addition to NF(a,b), both NF_2 and F are products of the NF_3/Ar microwave discharge. Rapid reaction of F with added H_2 produces atomic hydrogen which then reacts with NF_2, via the abstraction reaction (1), to generate more NF(a). These observations are also in accord with those reported by Herbelin and Cohen.[7] Figure 2 shows the dependence of the NF(a→X) emission upon the H_2 flow rate. Note that as H_2 is added, the [NF(a)] increases, goes through a peak, and then reaches an asymptotic limit at high H_2 flows. These conditions of high H_2 flow rate obtained in our kinetic measurements. The motivation for adding a large excess of H_2 with respect to NF_3 was to react away any free F and NF_2 produced in the discharge. In addition, by injection of a large excess of H_2 in the formation region of NF(a), subsequent addition of smaller amounts of undissociated H_2 further downstream would have minimal effect on the NF(a) number density. All removal then could be attributed to H atoms.

The point in Figure 2 at which the [NF(a)] reaches a plateau, which is independent of further increases in H_2, is most likely the point at which all F generated in the discharge has been consumed, i.e., $[H_2]_0 \sim [F]_0$. In this case the discharge produces approximately four F atoms for every five NF_3 molecules introduced to the discharge. We estimated $[NF_2]_0$ from kinetic modeling of profiles of NF(a), $N(^2D)$, and $N_2(B)$.[11] We found the ratio $[NF_2]_0/[F]_0 \sim 0.5$, from which we infer a yield of NF_2 from NF_3 of about 40%. Note that the discharge runs at low power, <10 W. Increasing the discharge power to 30 W drastically reduces [NF(a)], indicating dissociation of NF_2 at the higher microwave powers. Another indication of this enhanced dissociation is our observation of $N(^4S)$ generation at the higher microwave powers.

Our approach appears to provide a relatively safe and efficient source of NF(a) for kinetic studies. Habdas et al.[16] recently showed that adding HN_3 to excess F atoms also provides a good chemical source for NF(a) kinetic studies. The advantage of our approach over that of Habdas et al. or that from direct addition of H to NF_2 is the elimination of handling hazardous chemicals such as HN_3 or N_2F_4.

H Atom Calibration Procedure. The chemiluminescent titration of H by NO was used to measure H atom number densities. The recombination reaction of H + NO produces HNO emission with four characteristic features at 627.2, 692.5, 762.5, and 796.5 nm.[17] We monitored the 692.5-nm peak with a Hamamatsu R955 photomultiplier tube (PMT) restricted to a 9-nm band-pass by an interference filter centered at 690.5 nm.

Clyne and Thrush[17] have shown that the HNO* emission intensity resulting from the three-body recombination H + NO + M → HNO* + M is described by

$$I_{HNO} = K[H][NO] \quad (4)$$

and is independent of total pressure over the range of 1–2.5 Torr. The proportionality constant, K, is determined by titrating H with NOCl as originally described by Clyne and Stedman.[18] The reaction sequence is

$$H + NOCl \rightarrow HCl + NO \quad (5)$$

$$H + NO + M \rightarrow HNO^* + M \quad (6)$$

followed by radiative emission from HNO*. When [H] > [NOCl], unreacted H combines with NO to produce the HNO* → HNO + $h\nu$ red afterglow.[17] When [NOCl] > [H], the glow is extinguished. To use this titration, one adds a metered flow of NOCl to an unknown flow of H while monitoring the HNO* emission. Equation 4 shows that $I/[NO]$ is proportional to [H]. Thus, in the calibration experiment, $I/[NOCl]_{added}$ is also proportional to [H]. Note that $[H] = [H]_0 - [NOCl]_{added}$ where $[H]_0$ is the atomic hydrogen number density in the absence of added NOCl. Therefore

$$I = K([H]_0 - [NOCl])[NOCl] \quad (7)$$

(16) Habdas, J.; Wategaonkar, S.; Setser, D. W. *J. Phys. Chem.* **1987**, *91*, 451.
(17) Clyne, M. A. A.; Thrush, B. A. *Discuss. Faraday Soc.* **1962**, *33*, 139.
(18) Clyne, M. A. A.; Stedman, D. H. *Trans. Faraday Soc.* **1966**, *62*, 2164.

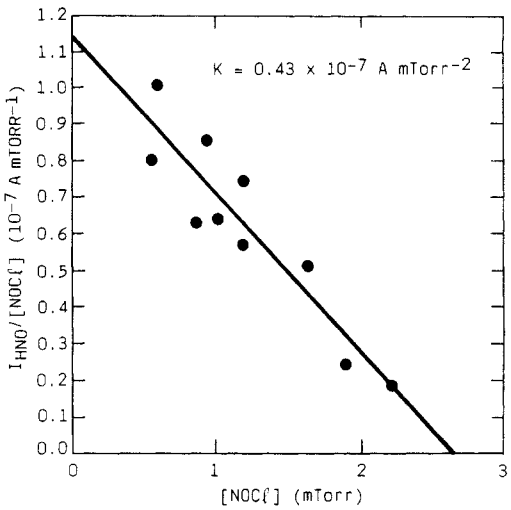

Figure 3. Typical data for H + NOCl titration.

A plot of $I/[NOCl]$ versus [NOCl] will be linear with a slope of K and an intercept on the abscissa of $[H]_0$. With K for our PMT/filter combination determined by this method, H atom number densities can be measured by adding known number densities of NO to the unknown H flow and monitoring the resultant HNO* chemiluminescence.

Although straightforward in principle, the NOCl calibration proved to be tedious with several subtle problems. Initial calibration plots were nonlinear with irreproducible K values. This problem apparently results from wall reactions. Clyne and Stedman[18] reported similar behavior on bare Pyrex walls. They postulated the following reaction sequence to explain this behavior:

$$H + NOCl \rightarrow HCl + NO \quad (5)$$

$$H + NO + M \rightarrow HNO^* + M \quad (6)$$

$$H + HCl \rightarrow H_2 + Cl \quad (8)$$

$$Cl + Cl \xrightarrow[\text{wall}]{} Cl_2 \quad (9)$$

$$H + Cl_2 \rightarrow HCl + Cl \quad (10)$$

The catalytic recombination of Cl on the wall forms Cl_2 which then consumes H via the rapid $H + Cl_2$ reaction. By treating their flow tube walls with phosphoric acid, which inhibits wall recombination of Cl, Clyne and Stedman's results became reproducible.

A section of our flow tube was uncoated Pyrex. This design permitted visual examination of chemiluminescence in the flow tube. Subsequent coating of this section with Teflon resulted in the calibration plots of $I/[NOCl]$ versus [NOCl] which were linear and which gave reproducible K's. Although the NOCl titration technique proved to be more difficult to use than anticipated, the titrations performed in the Teflon-coated flow tube gave satisfactory results.

Figure 3 shows a typical plot of $I/[NOCl]$ as a function of added [NOCl] using the fully coated reactor. An average of five calibration runs at various conditions yielded a proportionality constant $K = 0.46 \times 10^{-7}$ A mTorr^{-1} with a standard deviation of 15%. With a known K one can add a known concentration of NO to the flow and determine [H] from $[H] = I_{HNO}/K[NO]$.

Another problem encountered was that the H atom production at a given microwave power and at a constant Ar/H_2 flow rate varied in time. Heating of the microwave cavity and discharge tube appears to have been the cause of this problem. The flow of compressed air which was forced through the cavity apparently provided insufficient cooling for uniform H atom production. Flowing the cooling air through an ice bath prior to introduction into the microwave cavity alleviated this difficulty. H atom production remained constant for at least a minute at any microwave power. Since only a few seconds was sufficient to measure both the NF(a→X) and HNO* emission intensities, this remedy was satisfactory. A further improvement might be realized using

the design of Ding et al.,[19] who used a fluid as a coolant.

In practice, the microwave power was held fixed and [H] variations were obtained by changing the H_2 flow rate. The hydrogen dissociation efficiency, however, diminished as $[H_2]$ increased. This fact and the previously described dependence of H atom production on the temperature of the microwave cavity make it imperative that [H] be measured for each H_2 flow. One cannot rely upon comparable conditions to give the same [H].

Results

The rate equation for NF(a) decay in the flow tube is given by

$$d[NF(a)]/dt = -(k_2[H] + k_w)[NF(a)] \quad (11)$$

where quenching of NF(a) by NF, HF, and undissociated NF_3 is neglected. The rate coefficient for NF(a) self-quenching is a matter of some current controversy. Koffend et al.[20] saw no evidence of self-quenching in their experiments and concluded the rate coefficient for this process was less than 10^{-13} cm^3 molecule^{-1} s^{-1}. Quiñones et al.[21] on the other hand observed a decay at high [NF(a)] in their discharge-flow study which led them to assign a rate coefficient of 2.2×10^{-12} cm^3 molecules^{-1} s^{-1} for this process. At the low number densities of NF(a) in these studies, $\lesssim 10^{12}$ molecules cm^{-3}, self-quenching should be unimportant whether or not it is fast. No one has measured a rate coefficient for the reaction between ground-state NF and NF(a), but spin and angular momentum conservation rules indicate that the favored channel is endoergic.[22] Koffend et al. report that the rate coefficient between NF(a) and NF_2 is slow, $k = 2.7 \times 10^{-16}$ cm^3 molecules^{-1} s^{-1}, and Quinoñes et al. measured a value of 3.0×10^{-15} cm^3 molecules^{-1} s^{-1} for the quenching of NF(a) by HF(v'=0). Those two species, therefore, can be neglected safely. Vibrationally hot HF does quench NF(a) somewhat more efficiently,[23] but the large number densities of H_2 in the reactor will quench out all HF vibrational energy in the upstream region of the flow reactor prior to the reaction zone.[24] The rate coefficient for NF_3 quenching of NF(a) is unknown, but generally NF_3 is an inefficient electronic quencher. Experimentally, we keep the initial NF_3 concentration low ($<10^{13}$ molecules cm^{-3}) and constant for each run. Thus, even if some quenching by NF_3 or discharge-produced species were present, it will be independent of changes in [H].

Neglecting wall collisions, the integrated rate equation (under pseudo-first-order conditions, [H] >> [NF(a)] becomes

$$[NF(a)]/[NF(a)]_0 = e^{-k_2[H](z/\bar{v})} \quad (12)$$

where z is the distance from the injector to the observation port and $\bar{v}$ is the bulk gas velocity in the flow tube. If the number density of H is much greater than that of NF(a), plots of ln [NF(a) chemiluminescence intensity] as a function of $[H](z/\bar{v})$ yield k_2, the desired rate coefficient. Because NF(a) is relatively inert to wall deactivation, it will have a planar radial number density gradient. The plug-flow approximation used here, therefore, is appropriate.

The [NF(a)] was monitored, therefore, as a function of added discharged H_2, holding all other flows constant. No detectable change in [NF(a)] was observed for any secondary H_2 flow without the discharge. Large changes (approximately an order of magnitude) could be observed when the secondary H_2 discharge was initiated.

Typical H atom number densities were $\gtrsim 10^{14}$ atoms cm^{-3} while the undischarged $[NF_3]$ (which represents the maximum possible [NF(a)] was 10^{12}–10^{13} molecules cm^{-3}. Thus, the pseudo-first-order condition with H in excess was satisfied.

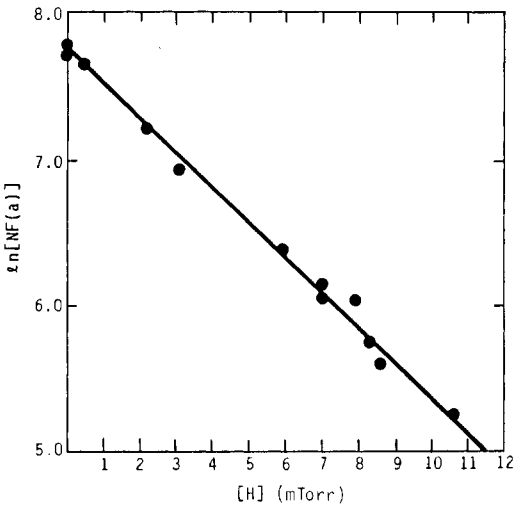

Figure 4. Plot of ln [NF(a)] as a function of added [H]. Total pressure for this run using Ar carrier gas was 1.79 Torr.

TABLE I: Compilation of Conditions for Measurement of H + NF(a) → Products Rate Coefficient[a]

pressure, Torr	flow velocity, cm s^{-1}	effective reaction time, 10^{-3} s	rate coefficient, cm^3 molecule^{-1} s^{-1}
1.49	2048	21.9	2.81×10^{-13}
1.79	1641	26.6	2.85×10^{-13}
0.91	3191	14.1	3.33×10^{-13}
1.61	1804	24.9	3.38×10^{-13}

[a] Buffer gas in all cases was Ar. Distance from H atom injector to observation port was 45 cm.

In practice, the peak NF(a→X) signal was monitored at 874.2 nm. Periodically we scanned the entire band to ensure the absence of any possible spectral interferences from N_2(B→A) and HF(v). The high H_2 flows used in these studies rapidly removed the N(^{2}D), which is the precursor of N_2(B) through reaction 3,[11,15] as well as quenching HF(v).[24]

Figure 4 is a sample plot of ln [NF(a)] as a function of [H]. These data yielded a rate coefficient of 2.9×10^{-13} cm^3 molecule^{-1} s^{-1}. Table I summarizes the results of measurements under several different sets of conditions.

The average of all runs, which were at room temperature, is $k = (3.1 \times 0.6) \times 10^{-13}$ cm^3 molecules^{-1} s^{-1}. The error represents the best estimate of the statistical and systematic uncertainties in the measurements. The dominant source of error is the H atom calibration. Although these experiments used a fixed injector, we do not think a large mixing correction is appropriate to our experimental conditions. Typical mixing corrections for most reagents in argon were on the order of 5–10 cm. H atoms will mix considerably more rapidly, however, because they diffuse much more quickly than other reagents. We saw no systematic variations in the measured rate coefficients when we varied reaction times.

Discussion

Our experimental value, $(3.1 \pm 0.6) \times 10^{-13}$ cm^3 molecule^{-1} s^{-1}, agrees quite well with the estimate of Cheah et al.[1] of 2.5×10^{-13} cm^3 molecule^{-1} s^{-1}. Their value is based upon computer modeling of temporal profiles of H in a flow containing H, H_2, and NF_2 and carried a substantial uncertainty regarding the electronic state of NF involved in the reaction. Subsequent modeling by Cheah and Clyne[2] of temporal profiles of N(^{2}D), N(^{4}S), and NF($a^1\Delta$) resulted in estimated rate coefficients for reaction 2 of 9×10^{-13} cm^3 molecule^{-1} s^{-1} assuming the bimolecular disproportionation of NF(a)

$$NF(a^1\Delta) + NF(a^1\Delta) \rightarrow N_2 + 2F \quad (13)$$

(19) Ding, A.; Karlaw, J.; Weiss, J. *Rev. Sci. Instrum.* **1977**, *48*, 1002.
(20) Koffend, J. B.; Gardner, C. E.; Heidner III, R. F. *J. Chem. Phys.* **1985**, *83*, 2904.
(21) Quiñones, E.; Habdas, J.; Setser, D. W. *J. Phys. Chem.* **1987**, *91*, 5155.
(22) Herbelin, J. M. *Chem. Phys. Lett.* **1976**, *42*, 367.
(23) Kwok, M. A.; Herbelin, J. M.; Cohen, N. In *Electronic Transition Lasers*; Steinfeld, J. J., Ed.; MIT Press: Cambridge, MA, 1976.
(24) de B. Darwent, B. *Natl. Stand. Ref. Data Ser.* **1970**, *31*.

had a rate coefficient of 7×10^{-11} and 4.5×10^{-13} cm^3 molecule^{-1} s^{-1} assuming reaction 13 to be negligibly slow. As we have already pointed out, whether or not reaction 13 proceeds facilely is subject to some controversy. Even Quiñones et al.'s[21] value for this rate coefficient, however, is substantially lower than the upper limit used in Cheah and Clyne's model calculations, so would probably tend to support their smaller value for k_2. Given that Cheah and Clyne's calibration of their resonance lamp used to determine $N(^2D)$ number densities was indirect, their estimated value for k_2 of $(4-6) \times 10^{-13}$ cm^3 molecule^{-1} s^{-1} also agrees adequately with our findings. Our measurement is a direct determination and should be preferred.

Throughout these studies [NF(a)] was always independent of $[H_2]$ added. No decrease in [NF(a)] could be seen even though sensitivity was more than adequate to see a 10% degradation. These observations establish an upper limit for H_2 quenching of NF(a) of 1×10^{-14} cm^3 molecule^{-1} s^{-1}. This can be compared to an earlier measurement of D_2 quenching of NF(a) by Kwok et al.[23] who reported a value of $k < 7 \times 10^{-14}$ cm^3 molecules^{-1} s^{-1}, and the recent measurements of Quiñones et al.,[21] who obtained $k = 6.4 \times 10^{-16}$ and 3.2×10^{-16} cm^3 molecule^{-1} s^{-1} for NF(a) quenching by H_2 and D_2, respectively.

Using vacuum-UV resonance fluorescence to monitor $N(^2D)$ and $N(^4S)$,[11] we have observed initial formation only of $N(^2D)$, with $N(^4S)$ appearing only later in the reaction, presumably as a result of $N(^2D)$ quenching. Cheah and Clyne[2,3] made similar observations and suggested that the primary product channel was to make $N(^2D)$. Absolute photometric measurements we have made of NF(a), $N(^2D)$, and $N_2(B)$ temporal profiles resulting from reactions 1 through 3, and which we shall report soon,[11] are fully consistent with a branching ratio for $N(^2D)$ formation in reaction 2 of unity. This is the result predicted by spin and orbital angular momentum correlation rules.[22]

Given that $N(^2D)$ is a key precursor for $N_2(A)$ formation via reaction 3, reaction 2 presents a kinetic bottleneck for this $N_2(A)$ generation scheme. Due to its relatively small rate coefficient, large H and NF(a) concentrations will be required in a generator to produce enough $N(^2D)$ to drive reaction 3. This is further exacerbated by the reactivity of $N(^2D)$ with generator surfaces and with other generation species such as NF_2, NF, H_2, and HF. However, the small value of k_2 at room temperature suggests the presence of an energy barrier, such that either elevated temperature or modest vibrational excitation of the NF(a) might provide a means for accelerating the reaction rate substantially.

Acknowledgment. We appreciate financial support from the Air Force Weapons Laboratory under Contract F-29601-84-C-0076. Insightful comments from our PSI colleagues, Dave Green, Bill Marinelli, and George Caledonia, benefited our efforts. Henry Murphy and Warren Savage's experimental assistance proved invaluable.

Registry No. H, 12385-13-6; NF, 13967-06-1.

Laser-Induced Fluorescence Spectroscopy of the $B^2\Pi$, $A^2\Delta$, and $C^2\Sigma^+$ States of the NS Radical

Jay B. Jeffries,* David R. Crosley, and Gregory P. Smith

Chemical Physics Laboratory, SRI International, Menlo Park, California 94025 *(Received: December 7, 1987)*

Laser-induced fluorescence has been used to study the $B^2\Pi$, $A^2\Delta$, and $C^2\Sigma^+$ excited states of the NS free radical in a low-pressure discharge flow system. Excitation scans were recorded exciting $v' = 0$–12 in B, $v' = 0$ and 1 in A, and $v' = 0$ in C. Numerous perturbations appear in excitation scans to the B state through anomalous Λ-doublet splittings and line intensities. Fluorescence spectra have been recorded through $v'' = 26$ in $X^2\Pi$ and have been used to determine vibrational term values in the ground state. Vibrational band transition probabilities have been measured for 236 bands in the B–X system, 10 bands in A–X, and 5 in C–X. The electronic transition moment for the B–X system is constant with internuclear distance, while that for C–X decreases with increasing distance.

Introduction

The NS radical possesses a large number of excited electronic states in the energy region 30 000–45 000 cm^{-1} above the ground $X^2\Pi$ state. These include both valence and Rydberg doublet states, as well as quartet states whose presence and spectroscopic constants have been inferred from perturbations of the doublets. This overall state structure has features in common with the more familiar, isovalent NO molecule, although in NS the valence states lie significantly lower in energy.

These states in NS are readily accessible to detection by laser-induced fluorescence (LIF) using tunable lasers together with standard nonlinear frequency conversion techniques. The NS radical is thereby amenable to two types of useful studies. The first type is collisional energy transfer, both internal (v,J,Ω) transfer within an electronic state, and state-specific quenching (total removal) and electronic-to-electronic transfer. For example, we have used the time dependence of LIF signals to investigate vibrational-level-specific total decay rates of the $B^2\Pi$ state.[1] The v' dependence of the decay rate varied with collision partner in both direction (increasing or decreasing) and magnitude, indicating interesting dynamic effects tied to the structure of the collider. In similar experiments on higher lying vibrational levels of $B^2\Pi$, the effects of perturbations on the collision-free decay and on collisional removal by N_2 were studied.[2] The many nearby electronically excited states in NS, having different electronic structure, and each accessible by laser excitation and fluorescence studies, make this radical a fertile ground for such collision studies.

The other type of study is the detection of NS in practical systems where it may play a chemical role. An example of this is the important area of combustion chemistry.[3] The radical had not previously been considered in this context, but we recently detected it in simulated coal flames,[4] that is, methane burning in oxygen with minor amounts (a few percent) of added NH_3 and H_2S. The detection was by LIF in the C–X system, and the absolute radical concentrations were deduced by using spectro-

(1) Jeffries, J. B.; Crosley, D. R. *J. Chem. Phys.* **1987**, *86*, 6839.

(2) Matsumi, Y.; Munakata, T.; Kasuya, T. *J. Phys. Chem.* **1984**, *88*, 264.

(3) Kaufman, F. *Proceedings of the Nineteenth Symposium (International) on Combustion*; The Combustion Institute: Pittsburgh, PA, 1982; p 1.

(4) Jeffries, J. B.; Crosley, D. R. *Combust. Flame* **1986**, *64*, 55.

0022-3654/89/2093-1082$01.50/0